

Hydrometeorological Research Centre of Russia

Some results of COSMO-RU7 convective instability forecasting verification

N.P. Shakina, E.N. Skriptunova, A.R. Ivanova

COSMO/CLM User Seminar DWD, Offenbach/Main, 05-07 March 2013

The characteristics of atmospheric convection as simulated by COSMO-RU7 are considered in connection with aviation weather forecasting.

Namely, during 2012, we developed a scheme to forecast thermal turbulence in the lower 3-km layer. It is known that such turbulence arises at the initial stages of convective development and then exists at its later stages.

With Cu and Cb clouds, thermal turbulence is always present in the sub-cloud air as well as in and between the clouds.

Apart from the zones of active convection, thermal turbulence can be associated with shallow convective mixing in the boundary layers, in particular – in those capped with stable layers (temperature inversions).

We intended to diagnose thermal turbulence (occurrence and intensity) from the output data of COSMO-RU7 model which is at present operatively used in the European parts of Russia and former USSR.

So, analysis was necessary of forecasting accuracy of convective instability and of mixed layer development.

An archive of the COSMO-RU7 output data is collected for that purpose during January to November 2012:

- initial fields at 00 and 12 UTC,
- forecasting fields with 12 and 24 h projections from 00 and 12 UTC.

By means of comparison the forecasting fields against the initial ones, accuracy is estimated of mixed and convectively unstable layers simulation.

The mixed layers develop due to convective mixing as the layers with neutral stratification, so that the temperature lapse rate is dry-adiabatic or, above the condensation level, moist-adiabatic.

The mixed layers are revealed as follows:

- temperature profile for the parcel lifting adiabatically from the lower level (1000 hPa) is calculated for every gridpoint both in the initial and forecasting fields;
- temperature difference, ΔT , between the lifting parcel and ambient air is calculated with 10 hPa step;
- the mixed layer top, H , is identified as that at which $|\Delta T| \leq 1^{\circ}$, while at the next step $|\Delta T| > 1^{\circ}$.

The obtained values of H are compared in the initial and forecasting fields, and occurrence frequencies of given H ranges are estimated.

The results show that

- in the initial fields, distribution of H occurrence frequencies is physically consistent: at 12 UTC, occurrence frequency of thin mixed layers is much lower and that of deep layer is higher than at 00 UTC.
- under 12-h and 24-h projections, the forecasting distribution of H is generally in a good agreement with that in the analysis (initial) fields; occurrence frequency of deep mixed layers is slightly overestimated, especially at 12 UTC, and percentage of thin mixed layers is slightly underestimated, as compared against analysis.
- in total, accuracy of mixed layer simulation is considered satisfactory. The mixed layers are those of light thermal turbulence.

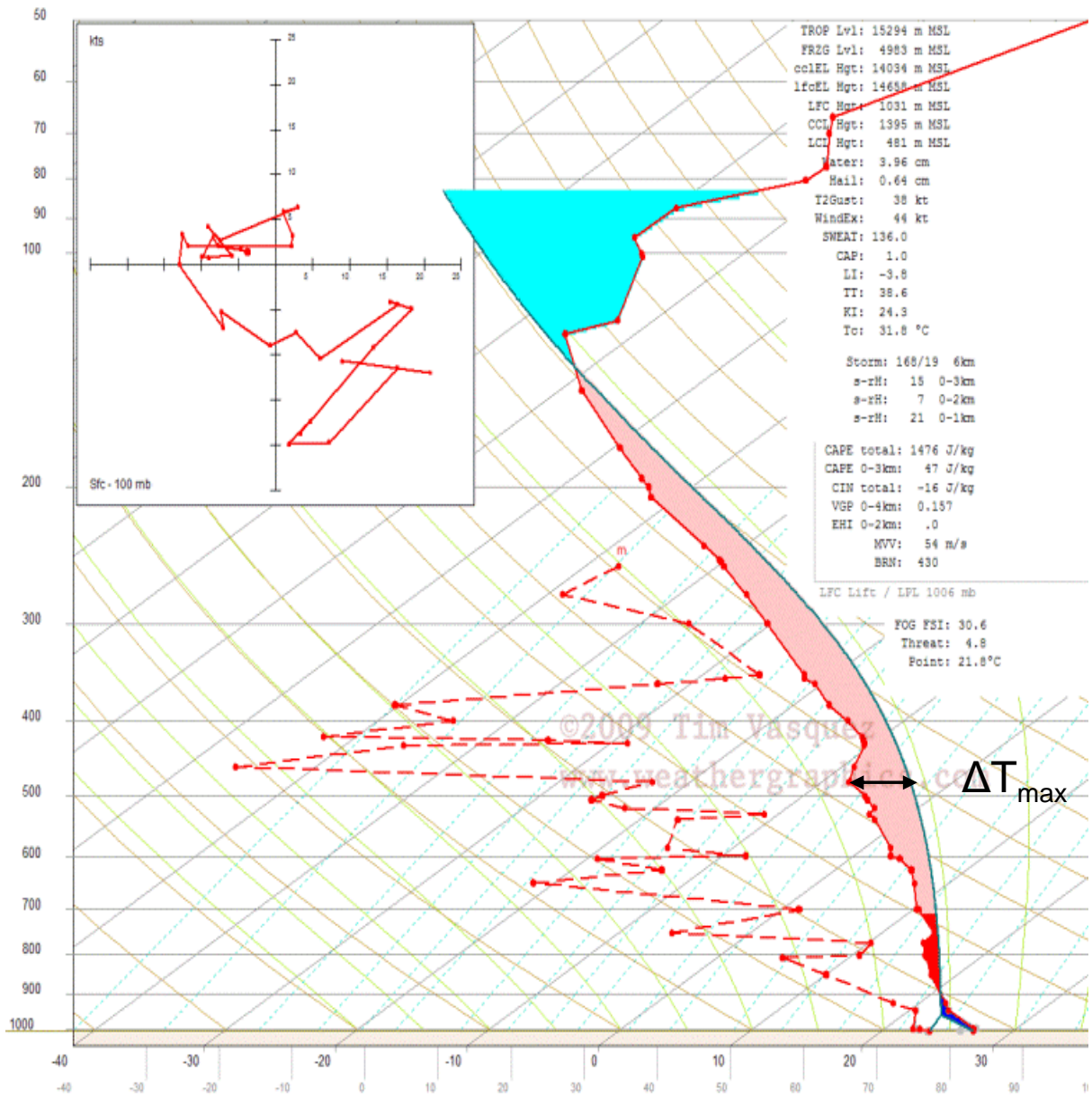
Then, the unstable layer simulation is estimated, as those of moderate and severe turbulence.

An empirical relationship exists between ΔT_{\max} in the unstable layers and turbulence intensity:

$\Delta T_{\max}, ^\circ\text{C}$	Turbulence intensity
1-3	light
4-6	moderate
≥ 7	severe

This relationship has been derived from the data of pilot reports in 1970ies.

ΔT_{\max} is maximum difference of temperature between the lifting parcel and the ambient air within the layer from 1000 to 400 hPa.



ΔT_{\max} forecasting accuracy is estimated by means of comparison of ΔT_{\max} occurrence frequency distribution in the initial and forecasting fields. In Tables below, the distributions are shown for the general sample (00 and 12 UTC, 11 months, including two projections (12 and 24 h)

Table 1
Occurrence frequencies of ΔT_{\max} in the initial fields
and in the forecasting fields with 12- and 24-h projections, general sample
(January to November 2012, 00 and 12 UTC)

ΔT_{\max} °C	Initial fields		12-h forecast		24-h forecast		Ratio (6):(2)
	Number of gridpoints	%	Number of gridpoints	%	Number of gridpoints	%	
1 - 2	17044991	53.7	12590407	59.1	12886309	60.6	0.76
2 - 3	6814992	21.5	4241622	19.9	4271404	20.1	0.63
3 - 4	3726512	11.8	2262744	10.6	2155636	10.1	0.58
4 - 5	1923555	6.1	1097378	5.2	1002072	4.7	0.52
5 - 6	1085898	3.4	509079	2.8	512039	2.4	0.47
6 - 7	604784	1.9	307497	1.4	251996	1.2	0.42
> 7	519752	1.6	213578	1.0	180004	0.9	0.35
Total	31720484	100.0	21311305	100.0	21259460	100.0	0.67
General sample	151039200	21.0	150550400	14.2	150794800	14.1	0.67
1	2	3	4	5	6	7	8

Table 2
Occurrence frequencies of ΔT_{\max} in the initial fields and in the forecasting fields with 12- and 24-h projections, general sample, 12 UTC

ΔT_{\max} °C	Initial fields		12-h forecast		24-h forecast		Ratio (6):(2)
	Number of gridpoints	%	Number of gridpoints	%	Number of gridpoints	%	
1 - 2	12642863	57.8	10496652	60.6	10657466	63.6	0.84
2 - 3	4615122	21.1	3294913	19.1	3203145	19.1	0.69
3 - 4	2398183	11.0	1774858	10.2	1558320	9.3	0.65
4 - 5	1100766	5.0	850487	4.9	674836	4.0	0.61
5 - 6	586050	2.7	469518	2.7	350823	2.1	0.60
6 - 7	304367	1.4	245088	1.4	177542	1.1	0.58
> 7	234446	1.0	181073	1.0	139412	0.8	0.59
Total	21881797	100.0	17312589	100.0	16761544	100.0	0.77
General sample	75519600	29.0	75764000	22.9	75030800	22.3	0.77
1	2	3	4	5	6	7	8

Table 3
Occurrence frequencies of ΔT_{\max} in the initial fields and in the forecasting fields with 12- and 24-h projections, general sample, 00 UTC

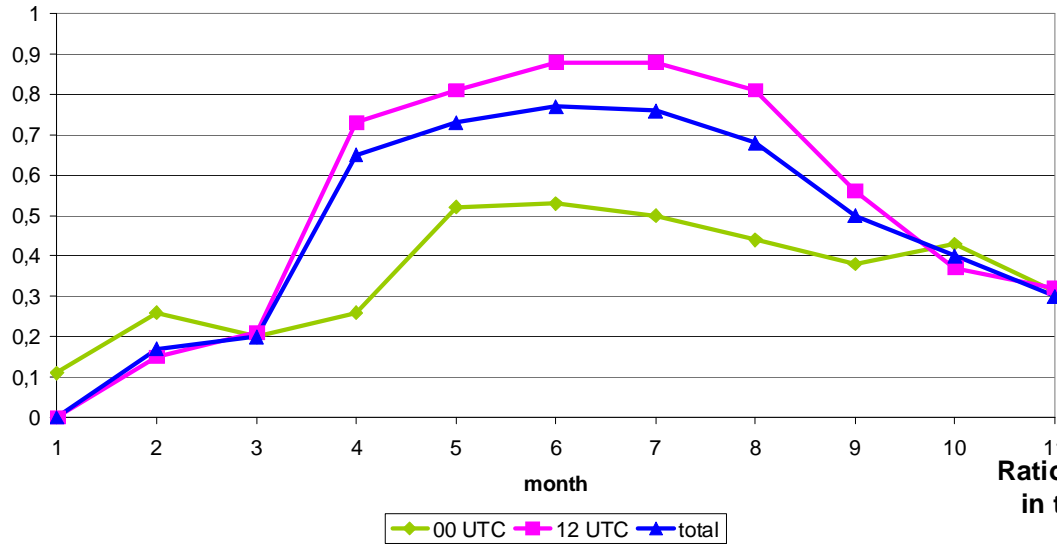
ΔT_{\max} °C	Initial fields		12-h forecast		24-h forecast		Ratio (6):(2)
	Number of gridpoints	%	Number of gridpoints	%	Number of gridpoints	%	
1 - 2	4402128	44.7	2093755	52.3	2228843	49.6	0.51
2 - 3	2199870	22.5	946709	23.7	1068259	23.6	0.48
3 - 4	1328329	13.5	487886	12.2	597316	13.3	0.45
4 - 5	822789	8.4	246891	6.2	327236	7.3	0.40
5 - 6	499848	5.0	128561	3.2	161216	3.6	0.32
6 - 7	300417	3.0	62405	1.6	74454	1.7	0.25
> 7	285306	2.9	32505	0.8	40592	0.9	0.14
Total	9838687	100.0	3998716	100.0	4497915	100.0	0.46
General sample	75519600	13.0	74786400	5.3	75764000	5.9	0.46
1	2	3	4	5	6	7	8

The conclusion from Tables 1-3:

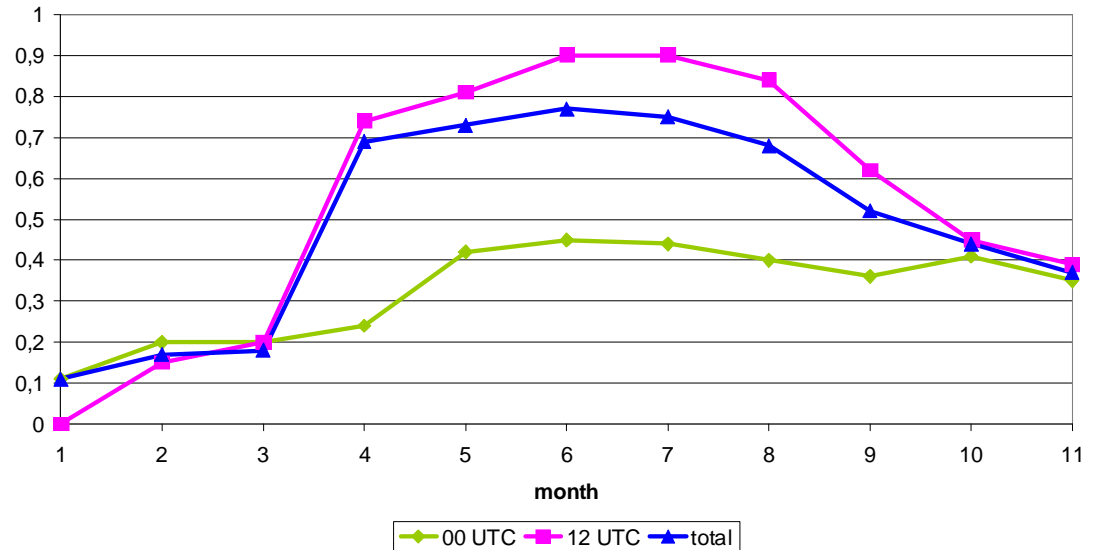
- total decrease of gridpoint numbers with convective instability in the forecasting fields;
- the decrease is mainly due to the forecasts valid for the night time (00 UTC): number of gridpoints with $\Delta T_{\max} > 1^{\circ}\text{C}$ is more than twice as high in the initial time than in 24 h forecast;
- underestimation is especially significant for deep convection (large ΔT_{\max}): for the forecasts valid at 00 UTC, $\Delta T_{\max} > 7^{\circ}\text{C}$ is about 7 times lower than in the initial fields (practically, for an order of magnitude).

It is interesting to estimate changes in ΔT_{\max} underestimation rate from month to month

Ratios of gridpoint numbers with convective instability in the forecasting and initial fields (12-h projection)



Ratios of gridpoint numbers with convective instability in the forecasting and initial fields (24-h projection)

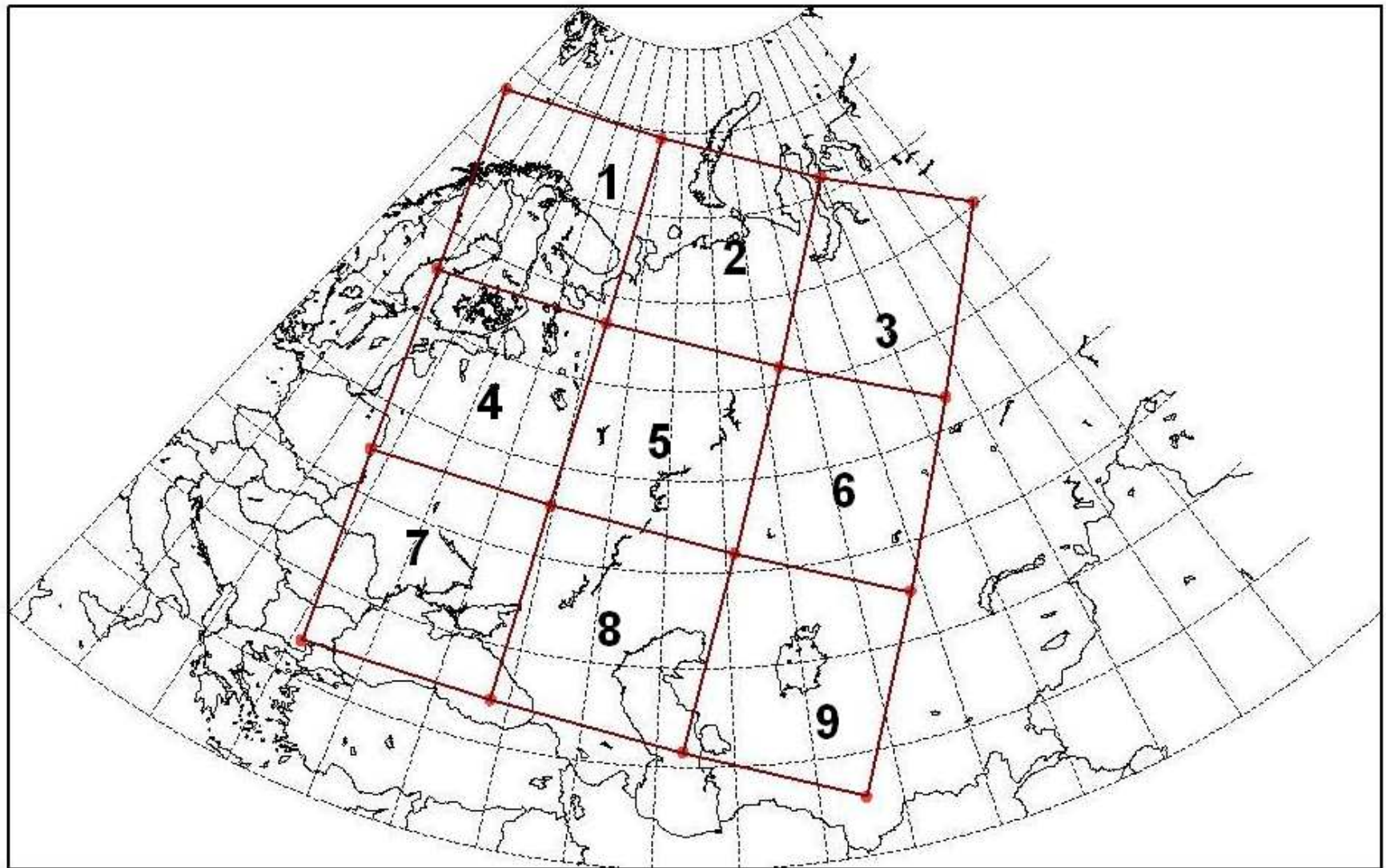


So, in winter and early spring (January to March) the forecasting number of gridpoints with convective instability is for an order of magnitude lower than in the analysis.

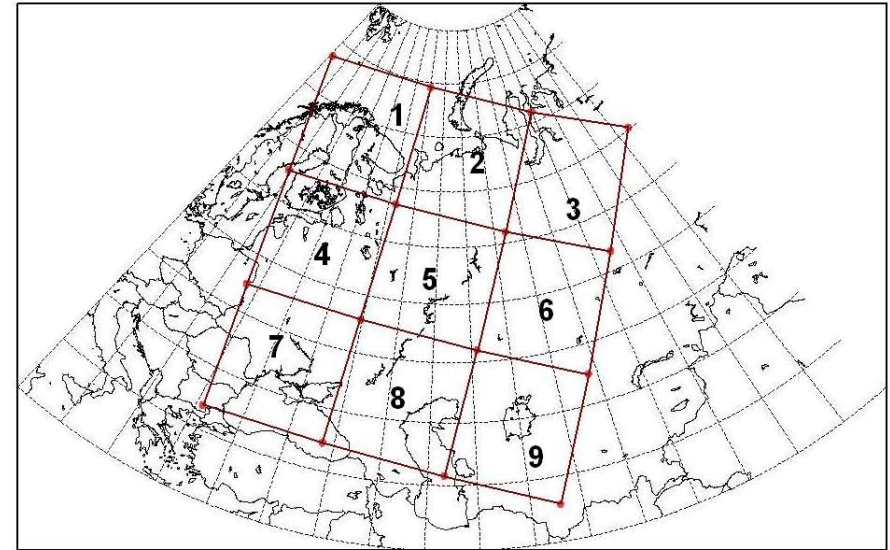
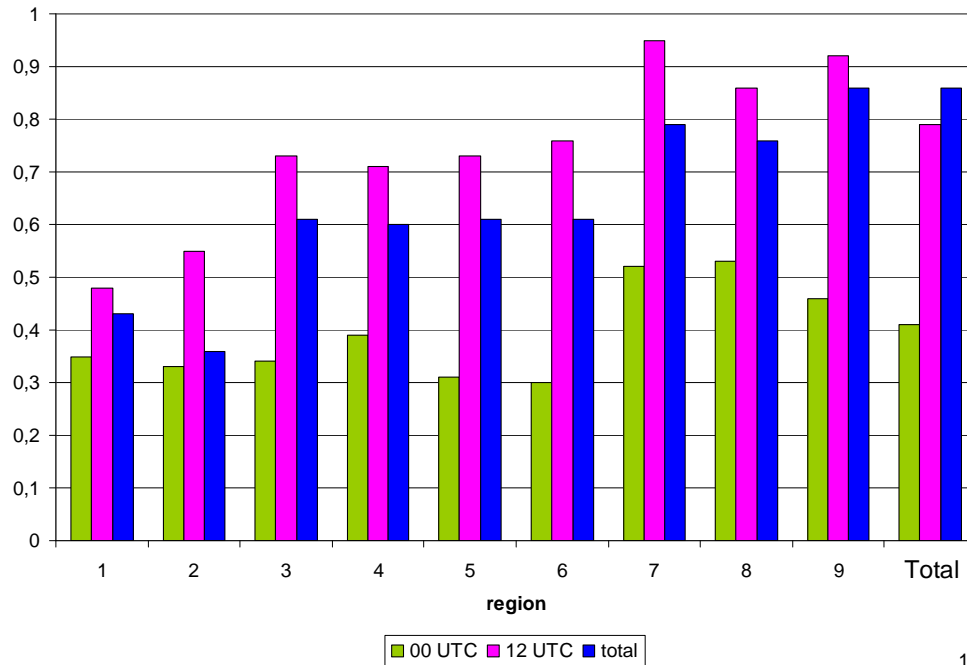
In the forecasting fields valid for 00 UTC, the ratio of forecasting and real (analysis) number of gridpoints with $\Delta T_{\max} > 1^{\circ}\text{C}$ is below 0,5 or but slightly higher than 0,5 during the whole period.

In the forecasting fields valid for 12 UTC, the ratio exceeds 0,7 from April to August, which can be considered a rather satisfactory result.

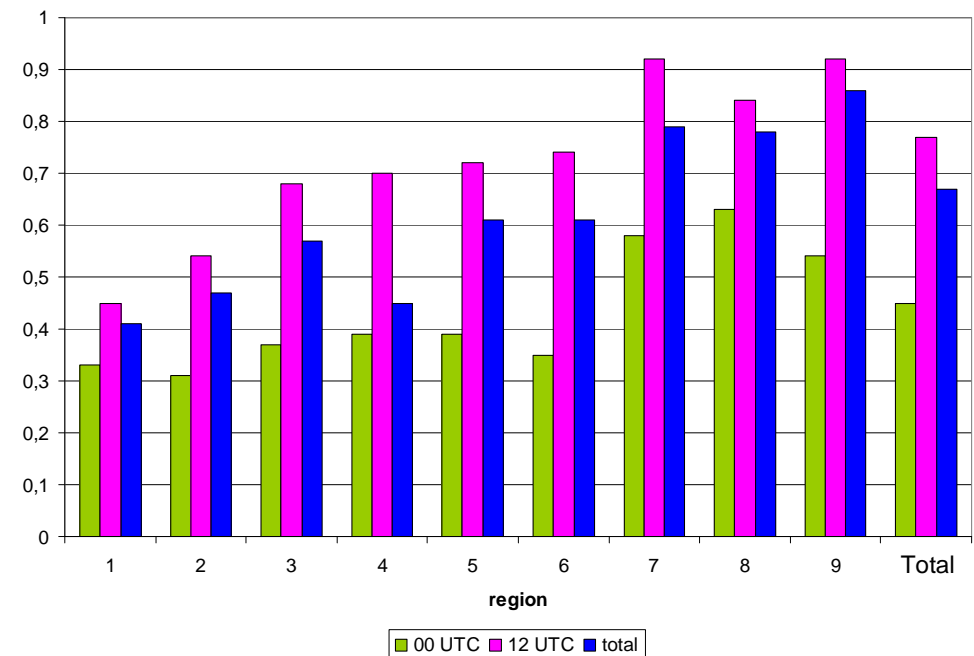
To estimate spatial distribution of ΔT_{\max} forecasting accuracy, the domain of COSMO-RU7 is divided into 6 regions:



Ratios of gridpoint numbers with convective instability in the forecasting and initial fields in different regions (12-h projection)



Ratios of gridpoint numbers with convective instability in the forecasting and initial fields in different regions (24-h projection)



For each region, the ratios of gridpoint numbers with convective instability in the forecasting and initial fields are estimated separately

So, in the southern belt (region 7-9) the forecasting efficiency, with respect to ΔT_{\max} , is the highest. Especially low ratios are typical for the forecasts valid for 00 UTC.

The conclusion is that COSMO-R7 underestimates significantly as well the total number of gridpoints with convective instability as the rate of convective instability, especially at the night time.

In concluding, I'd like to notice that non-standard verification, that is, estimation of physically consistent quantities derived from the direct output data, can give useful results.

In this way, sometimes special features can be revealed of the model fields, which cannot be found with standard verification procedure.

Thank you!